CLH-3, a ClC-2 anion channel ortholog activated during meiotic maturation in *C. elegans* oocytes

Eric Rutledge*, Laura Bianchi‡, Michael Christensen*§, Christoph Boehmer*, Rebecca Morrison*, Adam Broslat*, Andrew M. Beld*, Alfred L. George, Jr.‡§, David Greenstein† and Kevin Strange*§

Addresses: Departments of *Anesthesiology, †Cell Biology, ‡Medicine, and §Pharmacology, Vanderbilt University Medical Center, Nashville, Tennessee 37232, USA.

Correspondence: Kevin Strange
E-mail: kevin.strange@mcmail.vanderbilt.edu

Received: **13 November 2000**
Revised: **13 December 2000**
Accepted: **2 January 2001**

Published: **6 February 2001**

Current Biology 2001, 11:161–170

0960-9822/01/$ – see front matter

Background: ClC anion channels are ubiquitous and have been identified in organisms as diverse as bacteria and humans. Despite their widespread expression and likely physiological importance, the function and regulation of most ClCs are obscure. The nematode *Caenorhabditis elegans* offers significant experimental advantages for defining ClC biology. These advantages include a fully sequenced genome, cellular and molecular manipulability, and genetic tractability.

Results: We show by patch clamp electrophysiology that *C. elegans* oocytes express a hyperpolarization- and swelling-activated Cl^- current with biophysical characteristics strongly resembling those of mammalian ClC-2. Double-stranded RNA–mediated gene interference (RNAi) and single-oocyte RT-PCR demonstrated that the channel is encoded by *clh-3*, one of six *C. elegans* ClC genes. CLH-3 is inactive in immature oocytes but can be triggered by cell swelling. However, CLH-3 plays no apparent role in oocyte volume homeostasis. The physiological signal for channel activation is the induction of oocyte meiotic maturation. During meiotic maturation, the contractile activity of gonadal sheath cells, which surround oocytes and are coupled to them via gap junctions, increases dramatically. These ovulatory sheath cell contractions are initiated prematurely in animals in which CLH-3 expression is disrupted by RNAi.

Conclusions: The inwardly rectifying Cl^- current in *C. elegans* oocytes is due to the activity of a ClC channel encoded by *clh-3*. Functional and structural similarities suggest that CLH-3 and mammalian ClC-2 are orthologs. CLH-3 is activated during oocyte meiotic maturation and functions in part to modulate ovulatory contractions of gap junction–coupled gonadal sheath cells.

Background

Members of the ClC superfamily of voltage-gated Cl^- channels have been identified in plants, yeast, eubacteria, archaebacteria, and various invertebrate and vertebrate animals [1]. While the function and regulation of most ClC channels are obscure, the conservation of ClC genes in widely divergent organisms suggests that they play important and fundamental physiological roles.

Nine ClC genes have been described in mammals. Knockout studies and the identification of disease-causing mutations indicate that mammalian ClC-1, ClC-5, ClC-Ka/K1, and ClC-Kb/K2 channels function in the regulation of membrane potential, Cl^- transport in intracellular vesicles, and epithelial Cl^- transport [1]. The physiological roles of other mammalian ClC channels are not well defined.

Mammalian ClC-2 is expressed widely and is activated by membrane hyperpolarization and cell swelling [2, 3]. The functions of ClC-2 are unknown, but it has been proposed to play roles in transepithelial Cl^- transport [4], intracellular Cl^- regulation [5, 6], and cell volume homeostasis [3].

Six ClC genes are present in the *C. elegans* genome [7, 8]. These genes have been termed termed *clh* (Cl^- channel homolog)*-1–6* [8, 9] or *CeClC-1–6* [7] and are representative of the three major subfamilies of mammalian ClC channels [1]. Green fluorescent protein [7, 8] and *lacZ* [9] reporter studies have demonstrated that *clh* genes are expressed in a variety of worm cell types. Deletion mutagenesis of *clh-1* has shown that this channel may be important in seam cell function and whole-animal osmoregulation [9]. The specific physiological functions of the other *C. elegans clh* genes are unknown.

Figure 1

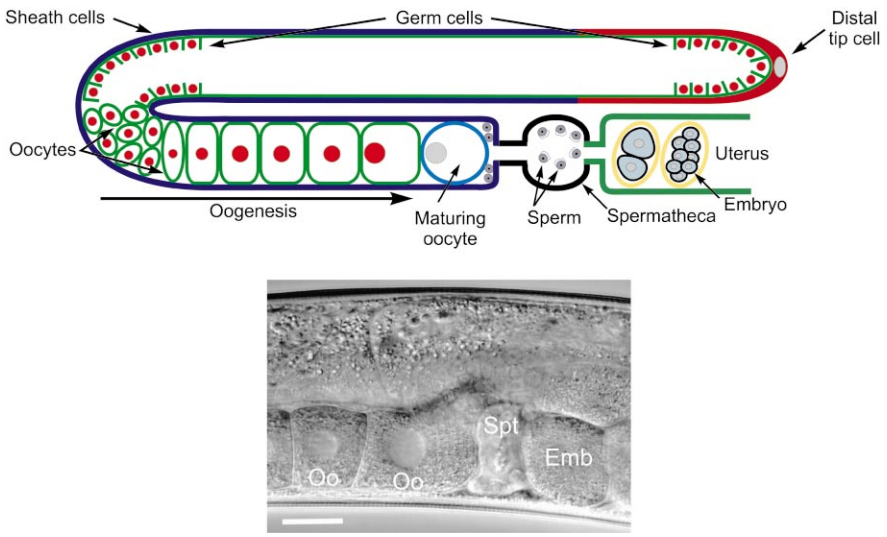

Schematic diagram and differential interference contrast micrograph of the adult hermaphrodite gonad. The following abbreviations were used: Oo, oocyte; Spt, spermatheca; Emb, embryo. The scale bar in the micrograph represents 20 μm.

C. elegans offers significant experimental advantages for characterizing ClC biology. Here we report that *C. elegans* oocytes express a hyperpolarization- and swelling-activated anion channel encoded by *clh-3*. CLH-3 has biophysical properties strikingly similar to those of mammalian ClC-2. The functional characteristics and primary structure indicate that CLH-3 and ClC-2 may be orthologs. Our results demonstrate that CLH-3 is activated during oocyte meiotic maturation and suggest that the channel participates in signaling pathways that modulate ovulatory contractions of myoepithelial sheath cells.

Results

C. elegans oocytes express a hyperpolarization- and swelling-activated anion current

The *C. elegans* hermaphrodite gonad consists of two U-shaped arms connected to a common uterus (Figure 1). Oocytes develop in the proximal region of the gonad and accumulate in a single row of graded developmental stages. The most differentiated oocyte is positioned next to the spermatheca, where it undergoes meiotic maturation and is then ovulated into the spermatheca and fertilized. Earlier-stage oocytes mature and are ovulated in a sequential, assembly line–like fashion [10, 11].

Late-stage oocytes not undergoing meiotic maturation were patch clamped in the whole-cell mode. Strong hyperpolarization activated a small, inwardly rectifying current (Figure 2a,c). Inward current was activated further and dramatically by oocyte swelling (Figure 2b,c). Swelling-induced current activation followed the time course of oocyte volume increase and could be reversed by oocyte shrinkage (Figure 2d).

Mean reversal potential (E_{rev}) for the swelling-induced current was -5 ± 1 mV ($n = 14$), which is close to the predicted value of -2 mV for a perfectly selective Cl^- channel. The replacement of bath NMDG with Na^+ had no significant effect on E_{rev} (Figure 3a), and this result demonstrated that the channel carrying the current is highly selective for anions over cations.

Replacement of bath Cl^- with Br^- or I^- shifted E_{rev} by -1 mV and $+21$ mV, respectively (Figure 2a). This finding indicated that the anion permeability sequence of the channel is $Cl^- \approx Br^- > I^-$. The current was unaffected by the disulfonic stilbene derivatives DIDS and DNDS (Figure 3b). However, NPPB, niflumic acid, Cd^{2+}, or Zn^{2+} inhibited current by 20%–90% (Figure 3b). Basal and swelling-induced currents were increased by acidic extracellular pH and were inhibited by alkaline conditions (Figure 3c).

Time-dependent activation of the current by hyperpolarization was fit by a biexponential function describing fast and slow components. The time constants for both components were reduced significantly by cell swelling (Figure 3d).

The inwardly rectifying Cl^- channel is encoded by *clh-3*

The characteristics of the oocyte current bear striking resemblance to those of mammalian ClC-2, a member of the ClC superfamily of anion channels [1]. This observation suggests that the channel is encoded by one or more of the six *C. elegans clh* genes. We carried out RNA interference (RNAi) [12] studies to test this hypothesis. Double-stranded RNA (dsRNA) complementary to *clh-1*, *clh-2*, *clh-4*, *clh-5*, and *clh-6* had no effect on swelling-induced current (Figure 4b). In contrast, *clh-3* dsRNA inhibited hyperpolarization (-100 mV)-activated current under

Figure 2

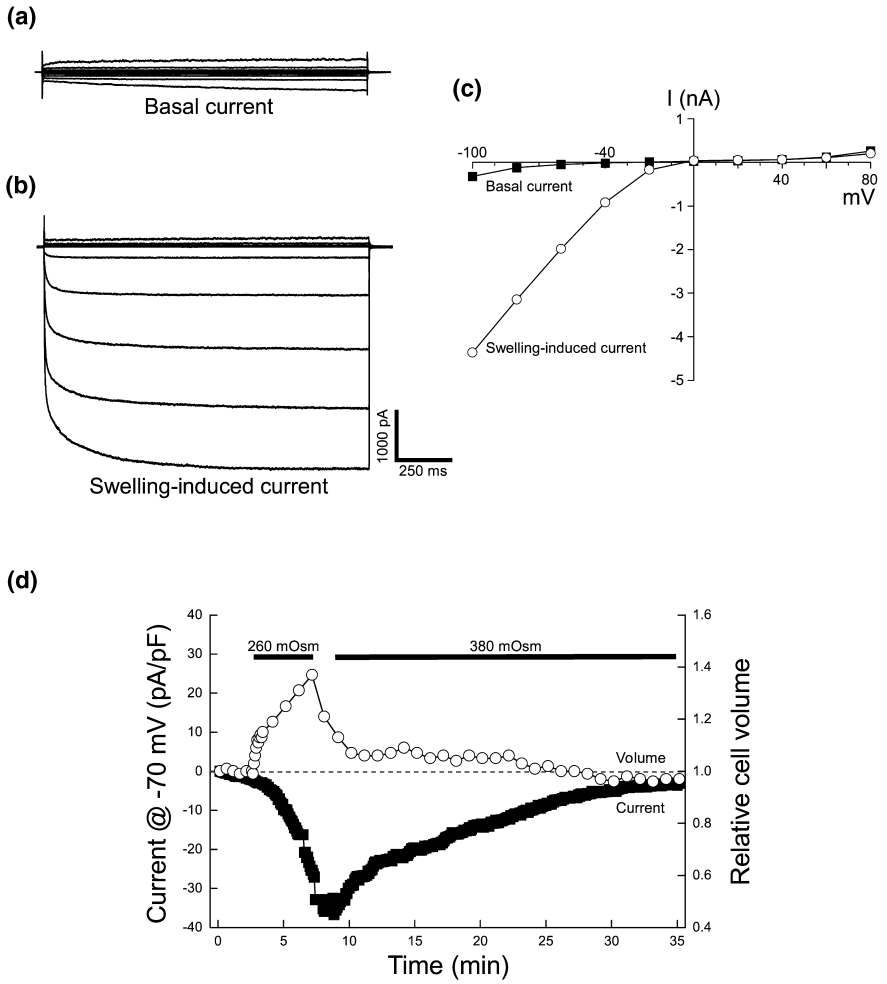

Activation of current in *C. elegans* oocytes. Stepping membrane voltage from −100 mV to +80 mV in 20 mV steps from a holding potential of 0 mV elicited **(a)** basal and **(b)** swelling-activated whole-cell currents. **(c)** Steady-state *I-V* relationships for the whole-cell currents shown in (a,b). **(d)** Relationship between current activation and cell volume in a single oocyte.

basal conditions by 82 ± 5% (mean ± S.E.; n = 4), and it inhibited swelling-induced current by >95% (Figure 4a,b). Single oocyte RT-PCR demonstrated that *clh-3* transcripts are present in oocytes (Figure 4c). Taken together, these results demonstrate that the oocyte channel is encoded by *C. elegans* gene *clh-3* (also termed *CeClC-3*; accession number AF173172; [7]).

CLH-3 plays no significant role in oocyte volume regulation

Regulation of CLH-3 and ClC-2 [3] by cell swelling suggests that the channels play roles in cell volume homeostasis. When exposed continuously to hypotonicity, intact oocytes swell and undergo a partial regulatory volume decrease (RVD) typical of many cell types. To assess the role of CLH-3 in oocyte osmoregulation, we quantified RVD in oocytes swollen by exposure to 260 mOsm Na^+-free (NMDG substitution) egg buffer. Oocytes were treated with 2 μM gramicidin 2 min prior to and during the hypotonic shock to ensure that membrane cation permeability was not rate limiting for RVD. Patch clamp and cell volume measurements in the presence of Na^+-containing egg buffer confirmed that gramicidin was effective in increasing cation permeability (data not shown). As shown in Table 1, the rate and extent of RVD were not significantly different in oocytes isolated from control, buffer-injected, and *clh-3* dsRNA–injected animals. Treatment of *clh-3* dsRNA oocytes with 10 mM $ZnCl_2$ had no significant inhibitory effect on RVD. The combination of RNAi (Figure 4) and Zn^{2+} exposure (Figure 3b) inhibits >99% of CLH-3 activity. The results shown in Table 1 demonstrate that CLH-3 plays no significant role in oocyte RVD following hypotonic swelling.

Swelling-induced and basal CLH-3 activity vary during oocyte development

In early patch clamp studies, we observed that the amount of swelling required to activate CLH-3 varied by as much as 50- to 60-fold between different oocytes. Furthermore, we found that there was a significant inverse relationship between oocyte size and apparent channel volume sensi-

Figure 3

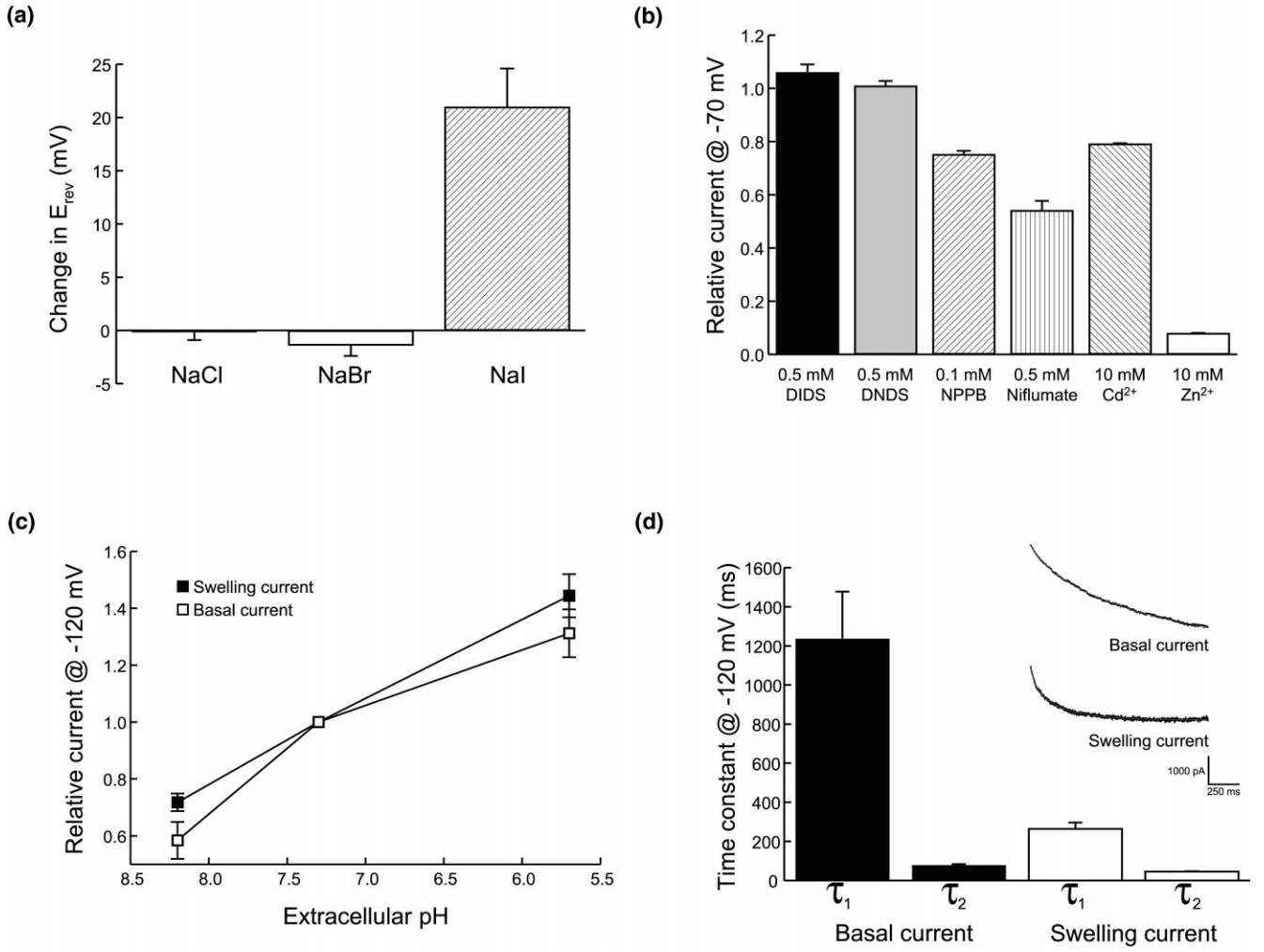

Biophysical characteristics of the inwardly rectifying anion current. **(a)** Ion selectivity. Change in reversal potential (E_{rev}) was measured after the complete replacement of the bath NMDG or Cl^- with the test ion. **(b)** Inhibitor sensitivity. Oocytes were exposed to each agent for 1–2 min while membrane potential was ramped from −80 mV to +80 mV. **(c)** Basal and swelling-induced currents are activated by acidic extracellular pH and inhibited by alkaline pH. **(d)** Hyperpolarization-induced current activation was fit by a biexponential function. Cell swelling significantly reduced ($p < 0.02$; paired samples) the time constants for voltage-dependent activation. Values shown in (a–d) are means ± S.E. (n = 3–6).

tivity; more cell swelling was required to trigger the current in small compared to large oocytes (Figure 5a).

Oocytes increase in volume approximately 200-fold over a 7–9 hr period prior to maturation and ovulation [10, 11]. The variability in the apparent volume sensitivity of CLH-3 as a function of cell size suggested that channel regulation changes during oocyte development. To test this hypothesis directly, we dissected a pair of oocytes, one at a late and one at an early stage of development, from single gonad arms and patch clamped them. As shown in Figure 5b, a smaller, earlier-stage oocyte always required substantially greater swelling to activate CLH-3 compared to its paired larger, later-stage sister oocyte.

The maximal swelling-induced current and rate of current activation were unchanged during oocyte development. CLH-3 currents in small, early-stage oocytes activated at similar rates and to similar extents as did larger oocytes at later stages of development (data not shown). These results suggest that the number of functional channels remains constant in the developmental stages examined.

The minimum cell volume at which a volume-sensitive channel activates is termed the "set point." It is conceivable that the set point of CLH-3 may be fixed at a volume close or equal to the size of a late-stage oocyte. In small, early-stage oocytes, more swelling would therefore be required to reach the set point and activate CLH-3. If this

Figure 4

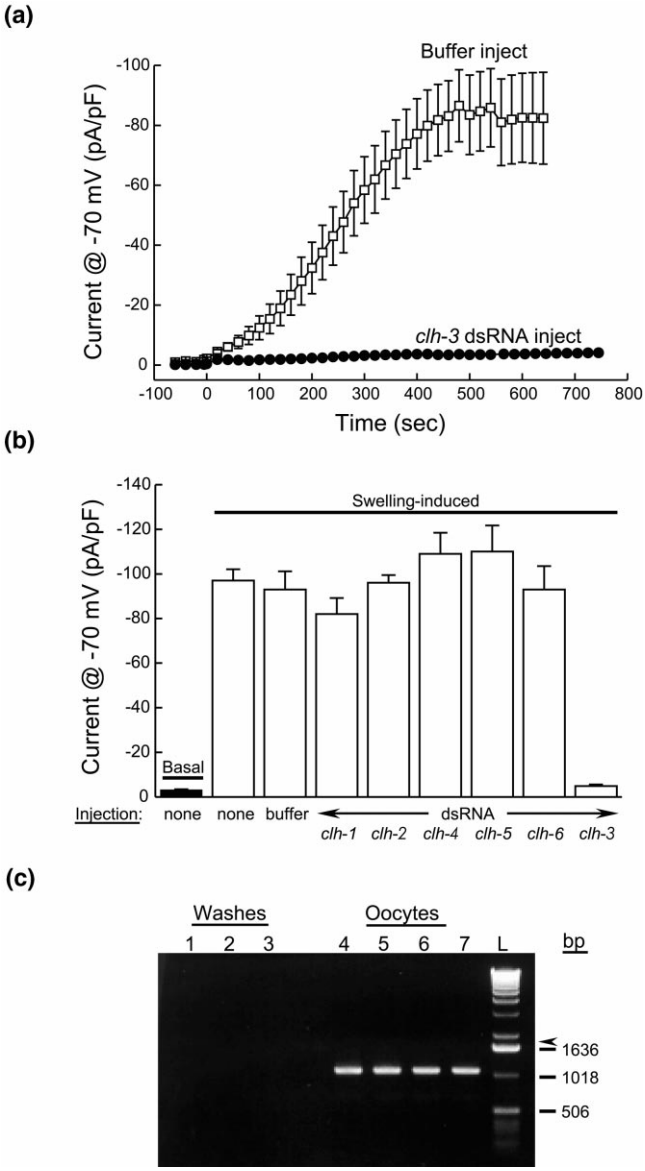

Disruption of whole-cell anion current by RNAi. **(a)** Swelling-induced current activation is inhibited by approximately 95% in oocytes isolated from worm gonads microinjected with *clh-3* dsRNA. **(b)** Microinjection of worm gonads with *clh-1*, *clh-2*, *clh-4*, *clh-5*, or *clh-6* dsRNA had no significant effect ($p > 0.05$) on swelling-induced current activation. For all dsRNA studies, swelling-induced currents were measured when they had reached steady-state levels 9–13 min after hypotonic shock. Whole-cell current in oocytes from *clh-3*–injected worms was recorded for up to 27 min with no indication of additional channel activation. Values in (a,b) are means ± S.E. (n = 5–34). dsRNA injections were performed 2–6 separate times for each construct used. **(c)** Detection of *clh-3* transcripts in single oocytes by nested RT-PCR. The expected product sizes for the amplification of *clh-3* cDNA and genomic DNA are 1096 bp and 1758 bp, respectively. The arrowhead shows the expected size of amplified genomic DNA.

Table 1

Regulatory volume decrease in oocytes

	Percent volume increase	Percent volume recovery at 30 min	Initial rate of recovery (Percent/min)
Control	24 ± 2	66 ± 4	−3.9 ± 0.3
Buffer inject	24 ± 2	36 ± 2	−4.2 ± 0.5
clh-3 dsRNA inject	29 ± 2	53 ± 7	−3.7 ± 0.5
clh-3 dsRNA inject +10 mM Zn^{2+}	26 ± 3	68 ± 13	−8.1 ± 1.6

Injection of buffer or *clh-3* dsRNA had no significant ($p > 0.05$) effect on the parameters measured. The exposure of *clh-3* dsRNA oocytes to 10 mM Zn^{2+} significantly ($p < 0.05$) increased the initial rate of volume recovery. This enhanced rate of volume recovery is most likely due to Zn^{2+}-induced inhibition of solute influx pathways. Values are means ± S.E. (n = 4–5).

hypothesis is correct, then it is conceivable that the channel might be constitutively activated in oocytes that have completed growth.

During late oogenesis when oocyte growth is complete, oocytes undergo meitoic maturation, which is marked by nuclear envelope breakdown (NEBD) (Figure 1) [10]. To test whether current was active in late-stage, full-grown oocytes, we isolated and patch clamped oocytes that had undergone NEBD in vivo. Whole-cell current was quantified within 15–20 s after we obtained whole-cell access. As shown in Figure 5c,d, a strongly inwardly rectifying current was detected in oocytes with NEBD but not in earlier-stage oocytes with intact nuclear envelopes. The amplitude of this current continued to increase until it reached a stable plateau level, typically 3–4 min after we obtained whole-cell access (e.g., see Figure 6c).

In NEBD oocytes, the replacement of bath Cl^- with Br^- or I^- shifted E_{rev} of the constitutively active current by −4 ± 1 mV and +21 ± 1 mV (n = 3), respectively. Whole-cell current was reduced by 82% ± 3% (n = 5) by 10 mM $ZnCl_2$, whereas 0.5 mM DIDS had no inhibitory effect (percent change in current with DIDS = 23% ± 12%; n = 5). Hyperpolarization-induced current activation at −120 mV was described by fast and slow time constants of 95 ± 6 ms and 712 ± 57 ms (n = 3), respectively. The channel carrying the current thus has the same anion selectivity, voltage sensitivity, and pharmacology as CLH-3 (see Figure 3). Furthermore, the shrinkage of oocytes by exposure to a hypertonic (385 mOsm) bath solution inhibited current amplitude 48 ± 14% (n = 4).

Data in Figure 5c demonstrate that CLH-3 is constitutively active in full-grown oocytes undergoing meiotic maturation. However, it is not clear from these results whether the channel is activated after completion of

Figure 5

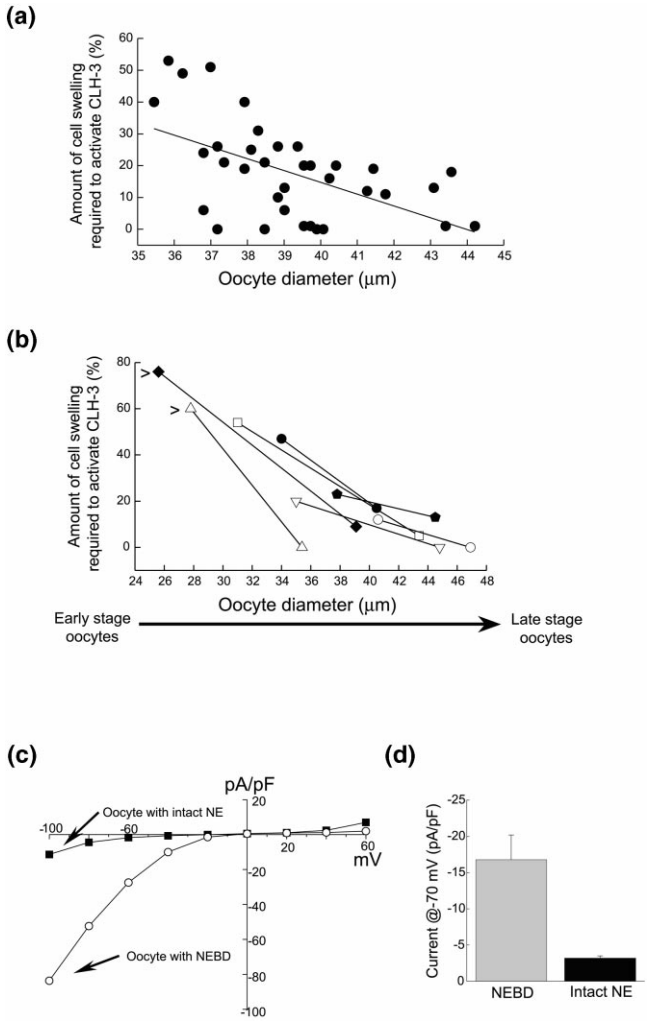

Developmental changes in CLH-3 activity. **(a)** Relationship between cell size and the amount of swelling required to activate CLH-3 in oocytes isolated from 35 gonads. The line is the least squares linear regression. The slope of the line is significantly different ($p < 0.0007$) from zero. **(b)** Relationship between oocyte developmental stage/cell size and the amount of swelling required to activate CLH-3 in paired oocytes isolated from single gonads. Each pair of symbols represents a pair of oocytes from a different gonad. The membrane seal was lost before current activation began in the two oocytes denoted by the greater-than (>) symbol. The cell swelling required to activate CLH-3 is therefore greater than the value plotted. **(c)** Steady-state *I-V* relationships and **(d)** mean ± S.E. whole-cell currents at −70 mV (right) in oocytes undergoing meiotic maturation (NEBD; n = 11) and oocytes with intact nuclear envelopes (NE; n = 34). Currents were measured within 15–20 s after whole-cell access was obtained.

Figure 6

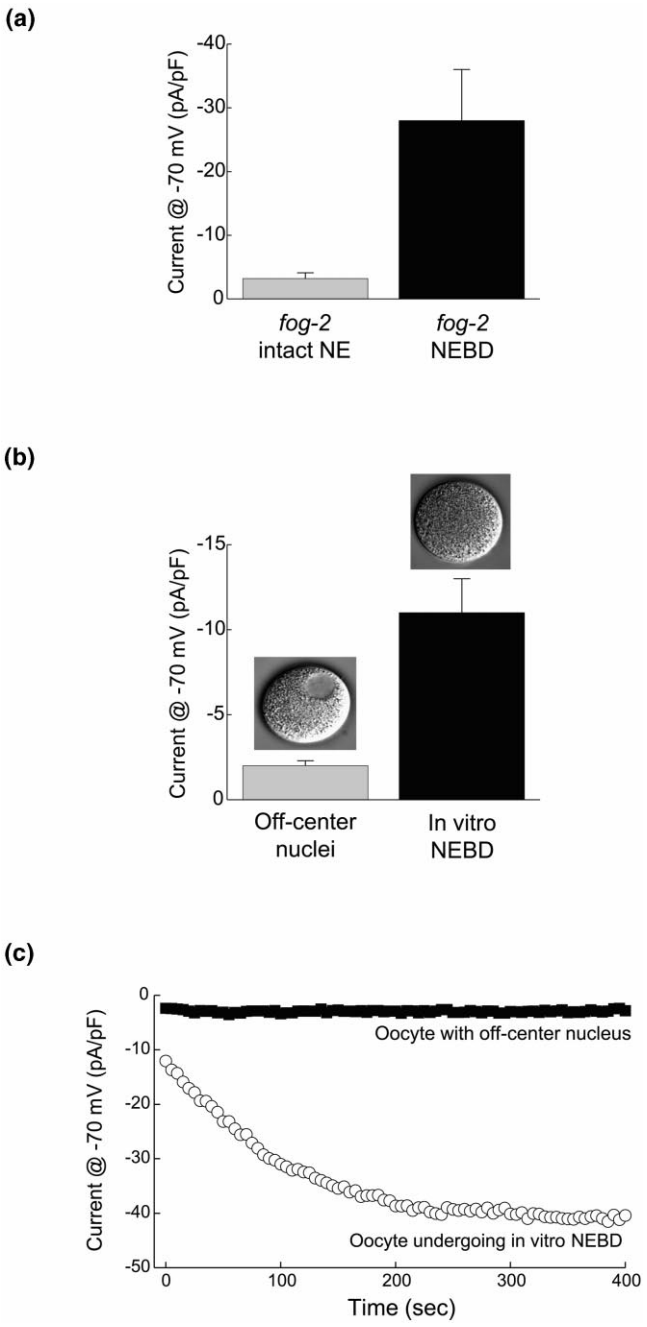

Activation of CLH-3 during meiotic maturation. **(a)** Mean ± S.E. whole-cell currents in full-grown nonmaturing (NE; n = 18) and spontaneously maturing (NEBD; n = 4) *fog-2* oocytes. **(b)** Mean ± S.E. whole-cell currents in wild-type oocytes with off-center nuclei (n = 5) and in wild-type oocytes that had undergone NEBD (n = 6) in vitro. Cell size did not change during in vitro maturation (see Results). **(c)** Whole-cell current in an oocyte with an off-center nucleus and in an oocyte undergoing in vitro maturation. No CLH-3 activation was detected in the nonmaturing oocyte. CLH-3 was active in the maturing oocyte and continued to activate for approximately 3 min after whole-cell access was obtained.

growth or during the maturation process. To address this issue, we carried out two additional sets of experiments.

Mutations in certain *C. elegans* sex determination genes, such as *fog-2*, block sperm production in hermaphrodites [13]. The presence of sperm is required for normal pro-

gression of meiotic maturation. Late-stage *fog-2* oocytes reach full-grown size, but they arrest in diakinesis for many hours to days [10]. Since ovulation is triggered by maturation, full-grown oocytes accumulate in the gonad of *fog-2* worms. We reasoned that if completion of growth activates CLH-3, then the channel should be active in late-stage *fog-2* oocytes. However, as shown in Figure 6a, full-grown *fog-2* oocytes show no basal CLH-3 current activity.

Meiotic maturation occurs in *fog-2* worms, but only sporadically at rates <1/40 of that of wild-type nematodes [10]. Despite this low maturation frequency, we were able to identify and patch clamp four *fog-2* oocytes undergoing maturation. Two of these oocytes underwent maturation in vivo, and two matured shortly after isolation from the gonad. As shown in Figure 6a, CLH-3 was constitutively activated in the maturing *fog-2* oocytes.

We also carried out a series of experiments on wild-type oocytes undergoing maturation in vitro. Shortly before maturation begins, the nucleus increases in size and migrates to the cell periphery ([10]; Figure 6b). Oocytes with centrally located nuclei were never observed to undergo maturation after isolation from the gonad. However, when oocytes with off-center nuclei were isolated and placed in a bath chamber, all of them underwent NEBD within 2–10 min (mean time to NEBD = 6.2 ± 1 min; n = 9). Cell volume did not change significantly during the maturation process; mean relative cell volume at the beginning of NEBD and 6 min later was 1.0 ± 0.01 and 1.01 ± 0.03 (n = 4 and 5), respectively.

In separate experiments, we patch clamped oocytes with off-center nuclei and oocytes that had undergone NEBD in vitro. As shown in Figure 6b,c, no current activity was detected in oocytes with off-center nuclei that had intact nuclear envelopes. However, in oocytes undergoing in vitro NEBD, we detected CLH-3 activity immediately upon obtaining whole-cell access. After we obtained whole-cell access, CLH-3 continued to activate until the current reached a stable plateau level (Figure 6c). Taken together, the results in Figure 6 demonstrate that CLH-3 is activated during meiotic maturation rather than after completion of oocyte growth.

RNAi of CLH-3 alters timing of sheath contractions

In the *C. elegans* gonad, meiotic maturation occurs only in the oocyte located immediately adjacent to the spermatheca ([10]; Figure 1). Once maturation begins, signaling events are triggered that induce a dramatic increase in sheath cell contractility and dilation of the distal spermatheca. Sheath ovulatory contractions drive the oocyte into the dilated spermatheca, where it is fertilized. This maturation and ovulation cycle repeats every 20–40 min [10]. Signals from the maturing oocyte control both sheath cell ovulatory contractions and spermatheca dilation [10, 14]. However, the precise mechanisms of intercellular signaling are incompletely understood.

Figure 7

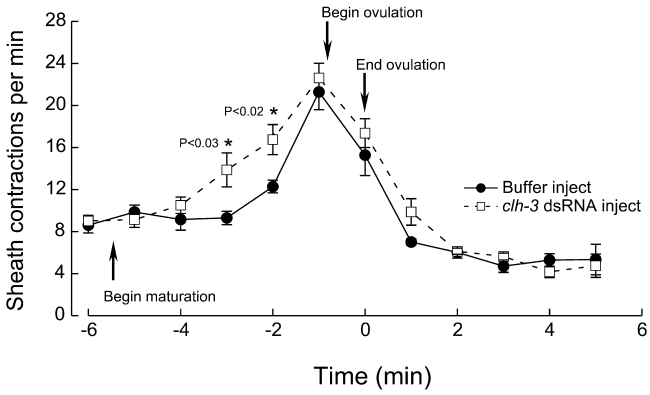

Sheath cell contractions during ovulatory cycles in buffer- and *clh-3* dsRNA–injected worms. Contractions were measured over 1 min time intervals. Values are means ± S.E. (n = 7, 8). dsRNA injections were performed 4 separate times. The timing of contractions in buffer-injected worms was similar to that of control animals (data not shown).

Activation of CLH-3 during meiotic maturation (Figure 6) suggested that the channel might function in signaling cascades that regulate the maturation process and/or fertilization events. To test this hypothesis, we determined the number of progeny produced, and we quantified the timing of processes associated with ovulation in worms injected with buffer or *clh-3* dsRNA. The mean ± S.E. number of progeny generated over a 36 hr period following buffer and dsRNA injection was 133 ± 9 (n = 34) and 129 ± 11 (n = 29), respectively, and the two were not significantly different ($p > 0.7$). Similarly, the timing of NEBD and cortical rearrangement, events that mark meiotic maturation, and entry of the fertilized egg into the uterus as well as embryo morphology were unaffected by CLH-3 RNAi (data not shown). Taken together, these results indicate that CLH-3 does not play essential roles in cell cycle progression, fertility, or embryo survival. However, it should be emphasized that residual channel activity remaining after RNAi may be sufficient for normal reproduction. Knockout of the channel gene may reveal reproductive and cell cycle control functions of CLH-3 that are not apparent in RNAi studies.

Prior to meiotic maturation, sheath cells contract weakly and intermittently at a basal rate of 7–8 contractions/min (Figure 7). Approximately 4–5 min after meiotic maturation begins, sheath cell ovulatory contractions are initiated. During this contractile cycle, both the force and rate of sheath contractions increase dramatically (Figure 7). Ovu-

latory contractions are inhibited rapidly after the oocyte completes its entry into the spermatheca ([10]; Figure 7).

The activation of CLH-3 in the maturing oocyte suggested that the channel might function to regulate ovulation. The disruption of CLH-3 expression by RNAi had no effect on the timing of spermatheca dilation and ovulation (data not shown). However, the knockdown of CLH-3 activity induced premature sheath cell ovulatory contractions. In *clh-3* dsRNA–injected animals, sheath contractions began approximately 2 min earlier than in control (data not shown) or buffer-injected worms (Figure 7). These results suggest that the activation of CLH-3 in the maturing oocyte functions as a negative or inhibitory regulator of sheath cell ovulatory contractions.

Discussion

The biophysical characteristics of CLH-3 as it is expressed in its native cellular environment bear striking resemblance to heterologously expressed mammalian ClC-2. ClC-2 exhibits a $Cl^- \geq Br^- > I^-$ anion selectivity sequence [2, 4, 15], is activated by cell swelling and hyperpolarization [2–4, 15–18], is relatively insensitive to disulfonic stilbene derivatives such as DIDS [2, 4, 15, 17], and is inhibited by NPPB, Cd^{2+}, and Zn^{2+} [4, 15, 17]. Voltage-dependent activation is enhanced by cell swelling [3, 15]. Acidic extracellular pH activates ClC-2, while alkaline pH inhibits the channel [15, 16]. Native ClC-2–like currents exhibit properties similar to those of heterologously expressed ClC-2 [5, 19–22]. Based on its functional properties and primary structure, which is 40% identical to ClC-2, we suggest that CLH-3 is a ClC-2 ortholog.

Nematodes are estimated to have diverged from other animals 600–1200 million years ago [23]. The striking conservation of the basic properties of CLH-3 and ClC-2 over such long evolutionary time spans suggests that the two channels may have similar physiological roles and regulatory mechanisms. One possible function of CLH-3 that is expected to be highly conserved is cell volume regulation, which is essential for the survival of all organisms. However, RNAi studies argue strongly that CLH-3 plays no significant role in the recovery of oocytes from hypotonic cell swelling (Table 1).

Similarly, there is no evidence that native ClC-2 channels play a role in cell volume control. Volume regulation is a ubiquitous and fundamental cellular homeostatic process. Consistent with this observation, virtually all vertebrate cells studied to date have been shown to express an outwardly rectifying, swelling-activated anion current that functions in cell volume regulation [24, 25]. In contrast, swelling-activated ClC-2–like currents have been reported in only a few vertebrate cell types (e.g., [19–22]). Furthermore, pharmacological studies in T84 cells demonstrated that ClC-2–like channels do not contribute to cell volume homeostasis [20].

Data shown in Figures 5 and 6 demonstrate that CLH-3 is activated during oocyte meiotic maturation. Both meiotic and mitotic cell cycle progression are cellular processes highly conserved in all eukaryotic organisms. The strong conservation of the basic properties of CLH-3 and ClC-2 may therefore reflect the existence of conserved cell cycle–dependent signaling pathways that regulate the activity of both channels. In this regard, it is particularly interesting to note that ascidian embryos express an inwardly rectifying Cl^- current similar to the CLH-3 and ClC-2 Cl^- current that is activated by cell swelling and hyperpolarization. The physiological functions and molecular identity of this channel are unknown, but current amplitude increases nearly 10-fold during mitotic cell cycle progression [26].

An interesting aspect of CLH-3 regulation is the apparent change in the volume set point of the channel as oocytes grow and develop (Figure 5). We have demonstrated recently that serine/threonine dephosphorylation triggers channel activation during both cell swelling and meiotic maturation (E. R. and K. S., unpublished data). It is possible that developmental changes in the activity of phosphorylation signaling pathways account for the change in the swelling sensitivity of CLH-3. Additional investigations of this possibility are clearly warranted, particularly in light of the fact that the ClC-2–like current in T84 cells is also regulated by protein dephosphorylation events [22].

In addition to the activation of CLH-3, a number of other physiological changes occur during meiotic maturation of *C. elegans* oocytes. Signals from the maturing oocyte trigger a dramatic increase in both the force and frequency of sheath cell contractions. These ovulatory contractions drive the maturing oocyte into the spermatheca [10]. The activation of CLH-3 during meiotic maturation suggested that the channel might modulate sheath cell function. Consistent with this hypothesis, we observed that sheath cell ovulatory contractions are triggered prematurely when CLH-3 expression is disrupted by RNAi (Figure 7). These results suggest that CLH-3 functions in a signaling pathway that modulates sheath cell contractile activity.

GFP reporter studies have not detected CLH-3 expression in sheath cells [7, 8] (L. B. and A. L. G., unpublished data). Thus, CLH-3 activity in the maturing oocyte most likely controls sheath cell function. Oocytes are coupled to sheath cells by gap junctions [11], which indicates that cell-to-cell communication may be mediated by chemical and electrical signals.

The signaling mechanisms that regulate sheath cell contraction are unknown. However, rhythmic muscle contrac-

tions responsible for the defecation cycle in *C. elegans* are controlled by intestinal epithelial cell IP_3 receptors and intracellular Ca^{2+} oscillations [27]. IP_3 receptors are expressed abundantly in sheath cells [27, 28], and this suggests that IP_3-regulated changes in intracellular Ca^{2+} could control sheath contractility.

The maintenance of Ca^{2+} signals triggered by IP_3 is critically dependent on Ca^{2+} influx via plasma membrane receptor-activated Ca^{2+} channels (RACCs) [29, 30]. Unlike voltage-activated Ca^{2+} channels, RACCs exhibit strong inward rectification due in part to depolarization-induced decreases in open probability [30]. Given the strong inward rectification of CLH-3 (Figure 2), we propose that activation of the channel during meiotic maturation depolarizes the oocyte and gap junction–coupled [11] sheath cell plasma membranes. If RACCs participate in sheath cell Ca^{2+} signaling, membrane depolarization will inhibit Ca^{2+} influx and sheath contraction. As maturation progresses, downregulation of CLH-3 activity, activation of other ion channels, or disruption of oocyte–sheath cell gap junction communication could repolarize sheath cells and initiate Ca^{2+} influx and contraction. Clearly, a full understanding of the signaling roles of CLH-3 requires detailed knowledge of the mechanisms by which sheath cell contractions are regulated.

Conclusions

In summary, we have identified by using physiological and molecular biological approaches a ClC anion channel that is activated during meiotic maturation in *C. elegans* oocytes. One of the physiological roles of CLH-3 is to modulate ovulatory contractions of myoepithelial sheath cells that are electrically coupled to oocytes via gap junctions [11]. The striking conservation of functional properties and primary structure suggest that CLH-3 is an ortholog of mammalian ClC-2. Our studies have provided unique and experimentally testable insights into the function and regulation of mammalian ClC-2 specifically and of ClC channels in general, as well as insights into the role of ion channels in controlling cell cycle–related processes.

Material and methods

Isolation of oocytes

The N2 (Bristol) and CB4108 *fog-2* (q71) [13] *C. elegans* strains were cultured at 25°C by standard methods. We isolated gonads by placing single nematodes in egg buffer (118 mM NaCl, 48 mM KCl, 2 mM $CaCl_2$, 2 mM $MgCl_2$, and 25 mM Hepes [pH 7.3, 340 mOsm]) and cutting them behind the pharyngeal bulb and in front of the spermatheca by using a 26 gauge needle. Isolated gonads were transferred to a patch clamp bath chamber. Late-stage oocytes were spontaneously released from the cut end of the gonad. We isolated early-stage oocytes by dissecting sheath cells away from the gonad with glass micropipettes under micromanipulator control.

Patch clamp recordings and oocyte volume measurements

Oocytes were allowed to attach to the cover slip bottom of a bath chamber mounted onto the stage of an inverted microscope. Patch electrodes were pulled from 1.5 mm outer-diameter silanized borosilicate microhematocrit tubes. Currents were measured with an Axopatch 200B (Axon Instruments) patch clamp amplifier by the use of a bath solution containing 116 mM NMDG-Cl, 2 mM $CaCl_2$, 2 mM $MgCl_2$, 25 mM Hepes, and 71 mM sucrose (pH 7.4, 340 mOsm) and a pipette solution containing 116 mM NMDG-Cl, 2 mM $MgSO_4$, 20 mM Hepes, 6 mM CsOH, 1 mM EGTA, 48 mM sucrose, 2 mM ATP, and 0.5 mM GTP (pH 7.2, 315 mOsm). Electrical connections to the amplifier were made with Ag/AgCl wires and 3 M KCl/agar bridges. Data acquisition and analysis were performed with pClamp 6 software (Axon Instruments).

We monitored changes in whole-cell current by ramping membrane potential from −80 to +80 mV at 80 mV/s every 5 s. Whole-cell currents and volume changes were measured simultaneously in single oocytes. Patch-clamped oocytes were visualized by video-enhanced differential interference contrast (DIC) microscopy. Oocytes have a spherical morphology, and relative cell volume change was determined as (experimental CSA/control CSA)$^{3/2}$, where CSA is the cell cross-sectional area measured at a single focal plane located at the point of maximum oocyte diameter. DIC images were recorded by a CCD camera on video tape, and CSA was measured offline by image processing. Volume regulation in intact oocytes was quantified with the same imaging methods.

RNA interference

Established methods were used for the synthesis of dsRNA for specific *clh* genes [12]. Briefly, DNA templates encoding regions of the open reading frames for each *clh* gene were obtained by PCR. Sense and antisense RNA were synthesized by T7 polymerase (MEGAscript, Ambion). Template DNA was digested with DNaseI, and RNA was purified by phenol/chloroform extraction and isopropanol precipitation. RNA size, purity, and integrity were assayed on denaturing agarose gels. To form dsRNA, we annealed sense and antisense RNA in potassium citrate buffer at 80°C for 3 min. Worms were injected in one gonad arm with at least 1,000,000 molecules of dsRNA or with a similar volume of potassium citrate buffer. Experiments were performed 20–24 hr after injection. The open reading frame locations of each dsRNA used were as follows: *clh-1*, 203–650 bp; *clh-2*, 1–610 bp; *clh-3*, 1–820 bp; *clh-4*, 2013–2873 bp; *clh-5*, 1–360 bp; and *clh-6*, 1–390 bp. dsRNA constructs shared no more than 50% identity with one another.

Single oocyte RT-PCR

Gonad arms were dissected in egg buffer as described above, were transferred through two separate 10 ml buffer washes, and were then placed in a disposable 0.25 ml bath chamber. After an oocyte was ejected, the gonad was removed, and the chamber was perfused with 50 ml egg buffer. Single washed oocytes were transferred by micropipette to 2 μl of distilled water in a PCR tube and were lysed by freeze-thawing. Samples of perfusate surrounding oocytes were also placed into PCR tubes. The volume transferred was approximately 2- to 3-fold greater than the fluid volume transferred with the oocyte. We performed nested RT-PCR to determine the presence of *clh-3* transcripts in oocytes. We had the primers flank DNA sequence containing five introns in order to distinguish the amplification of cDNA from that of genomic DNA.

Progeny counts

Young adult hermaphrodites containing 0–5 embryos were injected with *clh-3* dsRNA or an equivalent volume of buffer. Injected worms were purged of already-formed embryos and were allowed to recover for 4 hr. The number of progeny produced was measured at 25°C by the serial transfer of individual parents to growth plates at 12 hr intervals for a total of 36 hr. Experiments were repeated three times, and the results were averaged to yield mean brood sizes.

Video microscopy analysis of gonad function

Worms were anesthetized in M9 buffer containing 0.1% tricaine and 0.01% tetramisole for 30–40 min and were placed on 2% agar pads as described previously [10]. Anesthetized worms were imaged by DIC microscopy, and images were recorded on video tape at approximately one-fifth video framing rates with a Princeton Instruments MicroMAX cooled CCD camera.

Statistical analysis

Data are presented as means ± S.E. Statistical significance was determined with Student's two-tailed *t* test for paired or unpaired means. In comparisons of three or more groups, statistical significance was determined by one-way analysis of variance. *p* values of ≤ 0.05 were taken to indicate statistical significance.

Acknowledgements

We thank Lou DeFelice, David Miller, Luis Reuss, and Michael Welsh for helpful advice and critical reading of the manuscript. This work was supported by a National Institutes of Health National Research Service Award to E. R. (GM20764), a National Kidney Foundation postdoctoral fellowship to L. B., and National Institutes of Health Grants to D. G. (R01 GM57173), A. G. (R01 AR44506), and K. S. (R01 DK51610 and P01 DK58212).

References

1. Waldegger S, Jentsch TJ: **From tonus to tonicity: physiology of ClC chloride channels.** *J Am Soc Nephrol* 2000, **11:**1331-1339.
2. Thiemann A, Gründer S, Pusch M, Jentsch TJ: **A chloride channel widely expressed in epithelial and non-epithelial cells.** *Nature* 1992, **356:**57-60.
3. Gründer S, Thiemann A, Pusch M, Jentsch TJ: **Regions involved in the opening of ClC-2 chloride channel by voltage and cell volume.** *Nature* 1992, **360:**759-762.
4. Schwiebert EM, Cid-Soto LP, Stafford D, Carter M, Blaisdell CJ, Zeitlin PL, *et al.*: **Analysis of ClC-2 channels as an alternative pathway for chloride conduction in cystic fibrosis airway cells.** *Proc Natl Acad Sci USA* 1998, **95:**3879-3884.
5. Smith RL, Clayton GH, Wilcox CL, Escudero KW, Staley KJ: **Differential expression of an inwardly rectifying chloride conductance in rat brain neurons: a potential mechanism for cell-specific modulation of postsynaptic inhibition.** *J Neurosci* 1995, **15:**4057-4067.
6. Enz R, Ross BJ, Cutting GR: **Expression of the voltage-gated chloride channel ClC-2 in rod bipolar cells of the rat retina.** *J Neurosci* 1999, **19:**9841-9847.
7. Schriever AM, Friedrich T, Pusch M, Jentsch TJ: **ClC chloride channels in *Caenorhabditis elegans*.** *J Biol Chem* 1999, **274:**34238-34244.
8. Nehrke K, Begenisich T, Pilato J, Melvin JE: ***C. elegans* ClC-type chloride channels: novel variants and functional expression.** *Am J Physiol* 2000, **279:**C2052-C2066.
9. Petalcorin MI, Oka T, Koga M, Ogura K, Wada Y, Ohshima Y, *et al.*: **Disruption of *clh-1*, a chloride channel gene, results in a wider body *of Caenorhabditis elegans*.** *J Mol Biol* 1999, **294:**347-355.
10. McCarter J, Bartlett B, Dang T, Schedl T: **On the control of oocyte meiotic maturation and ovulation in *Caenorhabditis elegans*.** *Dev Biol* 1999, **205:**111-128.
11. Hall DH, Winfrey VP, Blaeuer G, Hoffman LH, Furuta T, Rose KL, *et al.*: **Ultrastructural features of the adult hermaphrodite gonad of *Caenorhabditis elegans*: relations between the germ line and soma.** *Dev Biol* 1999, **212:**101-123.
12. Fire A, Xu S, Montgomery MK, Kostas SA, Driver SE, Mello CC: **Potent and specific genetic interference by double-stranded RNA in *Caenorhabditis elegans*.** *Nature* 1998, **391:**806-811.
13. Schedl T, Kimble J: ***fog-2*, a germ-line-specific sex determination gene required for hermaphrodite spermatogenesis in *Caenorhabditis elegans*.** *Genetics* 1988, **119:**43-61.
14. Clandinin TR, Demodena JA, Sternberg PW: **Inositol trisphosphate mediates a RAS-independent response to LET-23 receptor tyrosine kinase activation in *C. elegans*.** *Cell* 1998, **92:**523-533.
15. Furukawa T, Ogura T, Katayama Y, Hiraoka M: **Characteristics of rabbit ClC-2 current expressed in *Xenopus* oocytes and its contribution to volume regulation.** *Am J Physiol* 1998, **274:**C500-C512.
16. Jordt SE, Jentsch TJ: **Molecular dissection of gating in the ClC-2 chloride channel.** *EMBO J* 1997, **16:**1582-1592.
17. Xiong H, Li C, Garami E, Wang Y, Ramjeesingh M, Galley K, *et al.*: **ClC-2 activation modulates regulatory volume decrease.** *J Membr Biol* 1999, **167:**215-221.
18. Park K, Arreola J, Begenisich T, Melvin JE: **Comparison of voltage-activated Cl^- channels in rat parotid acinar cells with ClC-2 in a mammalian expression system.** *J Membr Biol* 1998, **163:**87-95.
19. Duan D, Ye L, Britton F, Horowitz B, Hume JR: **A novel anionic inward rectifier in native cardiac myocytes.** *Circ Res* 2000, **86:**E63-E71.
20. Bond TD, Ambikapathy S, Mohammad S, Valverde MA: **Osmosensitive Cl^- currents and their relevance to regulatory volume decrease in human intestinal T84 cells: outwardly vs. inwardly rectifying currents.** *J Physiol* 1998, **511:**45-54.
21. Carew MA, Thorn P: **Identification of ClC-2-like chloride currents in pig pancreatic acinar cells**. *Pflugers Arch* 1996, **433:**84-90.
22. Fritsch J, Edelman A: **Osmosensitivity of the hyperpolarization-activated chloride current in human intestinal T84 cells.** *Am J Physiol* 1997, **272:**C778-C786.
23. Blaxter M: ***Caenorhabditis elegans* is a nematode.** *Science* 1998, **282:**2041-2046.
24. Strange K, Emma F, Jackson PS: **Cellular and molecular physiology of volume-sensitive anion channels.** *Am J Physiol* 1996, **270:**C711-C730.
25. Okada Y: **Volume expansion-sensing outward-rectifier Cl^- channel: fresh start to the molecular identity and volume sensor.** *Am J Physiol* 1997, **273:**C755-C789.
26. Block ML, Moody WJ: **A voltage-dependent chloride current linked to the cell cycle in ascidian embryos.** *Science* 1990, **247:**1090-1092.
27. Dal SP, Logan MA, Chisholm AD, Jorgensen EM: **The inositol trisphosphate receptor regulates a 50-second behavioral rhythm in *C. elegans*.** *Cell* 1999, **98:**757-767.
28. Baylis HA, Furuichi T, Yoshikawa F, Mikoshiba K, Sattelle DB: **Inositol 1,4,5-trisphosphate receptors are strongly expressed in the nervous system, pharynx, intestine, gonad and excretory cell of *Caenorhabditis elegans* and are encoded by a single gene (*itr-1*).** *J Mol Biol* 1999, **294:**467-476.
29. Barritt GJ: **Receptor-activated Ca^{2+} inflow in animal cells: a variety of pathways tailored to meet different intracellular Ca^{2+} signalling requirements.** *Biochem J* 1999, **337:**153-169.
30. Parekh AB, Penner R: **Store depletion and calcium influx**. *Physiol Rev* 1997, **77:**901-930.